Patrick Champagne

MAE 598: Applied Computational Fluid Dynamics

Project 4

Statement on Collaboration: No Collaboration

Task 1

In this task, I was asked to model the flow over a cylinder and two ellipses. In this case, the cylinder and ellipses were placed in a 2-D domain full of water with an inlet velocity of 3.5 cm/s. Standard values from the Fluent Database were used. The standard laminar model was used as well. The mesh used for all parts of this task has a resolution of 0.005m. This mesh is displayed in Figures 5 and 6. This simulation was run for five minutes with a timestep of 0.25s. The simulation was run for 1200 timesteps at 20 iterations per timestep.

Part a)

i) The Reynolds Number for this case was calculated using the following equation:

$$Re = \frac{\rho u L}{\mu} = \frac{998.2 * 0.035 * 0.1}{0.001003} = 3483.3$$

Where L is the diameter of the cylinder (0.1m) and u is the flow velocity (0.035 m/s).

ii) Figures 1, 2, and 3 contain contour plots of Static Pressure, y-velocity, and stream function for the case of flow over a cylinder. These plots also show the two-dimensional computational domain.
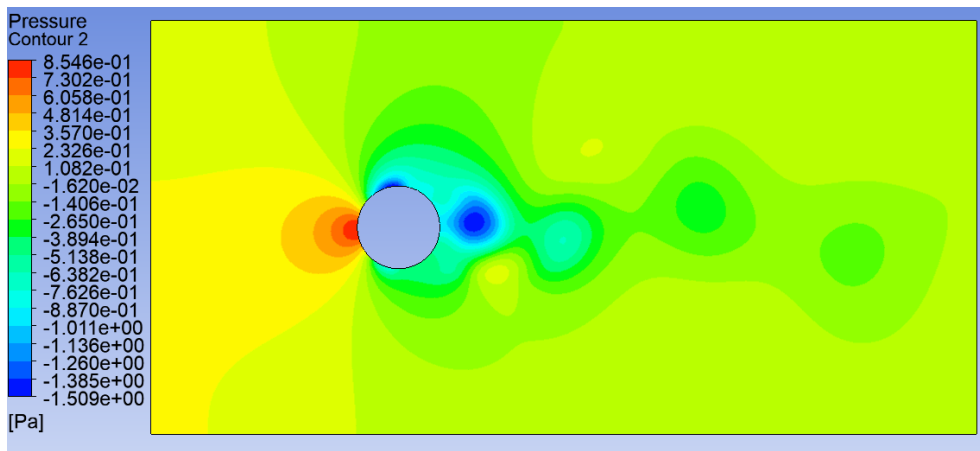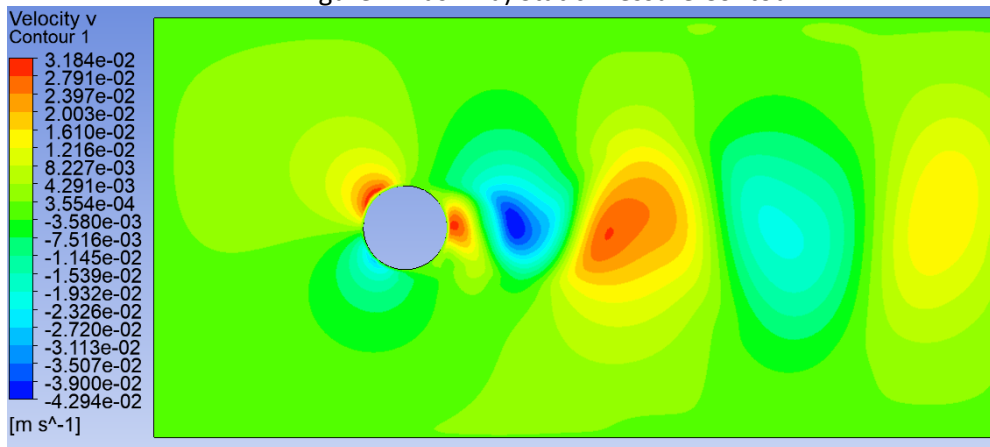

Figure 1. Task 1 a) Static Pressure Contour

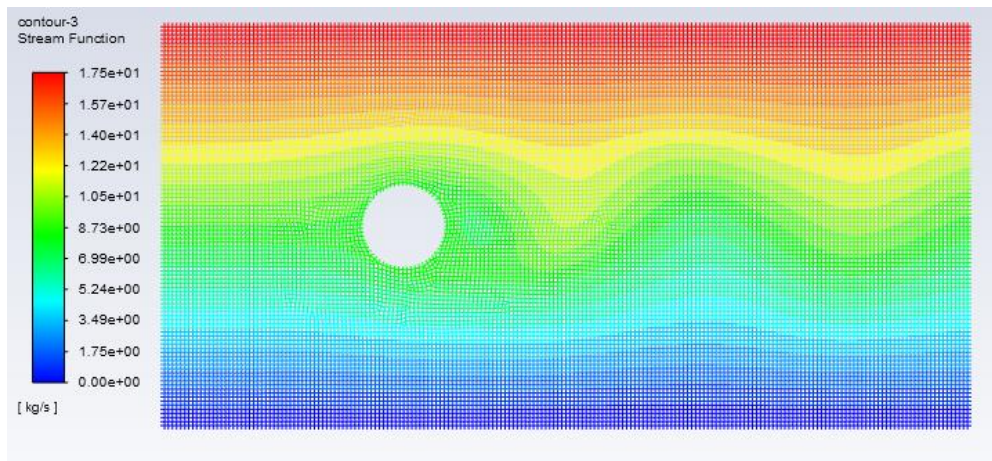Figure 2. Task 1 a) y-Velocity Contour

Figure 3. Task 1 a) Stream Function Contour

These figures show the behavior of the flow over the cylinder. It is clear from these plots that the flow is not steady and that there are oscillations in the flow. These plots, along with the line plots of lift force, show that the flow is not steady.

iii) Figure 4 shows the line plot of lift force on the cylinder over the last three minutes of the five-minute simulation. For the deliverables in this report, the "Lift Force" report was used in Fluent. This is Option 1 as listed in the addendum to this project. As predicted by the contours, the flow, and therefore lift force, are unsteady. The oscillations in lift force have an amplitude of **0.067275 N** and a period of **11s.**
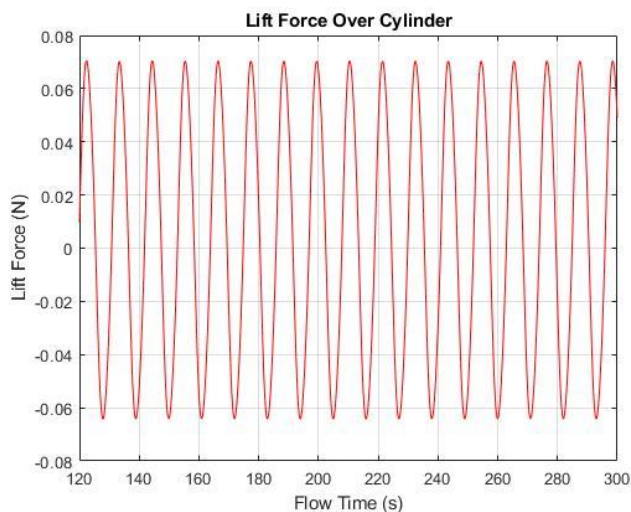

Figure 4. Task 1 a) Lift Force vs. Time

Part b)

In this part of Task 1, part a) was repeated with ellipses instead of a cylinder. In run 2, an ellipse with a major axis in the *y*-direction was used, while run 3 analyzes an ellipse with a major axis in the *x*-direction.

Figures 7 and 8 show lift force vs. time for the last three minutes of the simulation as in Figure 4. As in run 1, the solutions are oscillatory. The lift force for **Run 2** has an amplitude of **0.1432 N** and a period of **12.75s**, while the lift force for **Run 3** has an amplitude of **0.03399 N** and a period of **9.25s.**
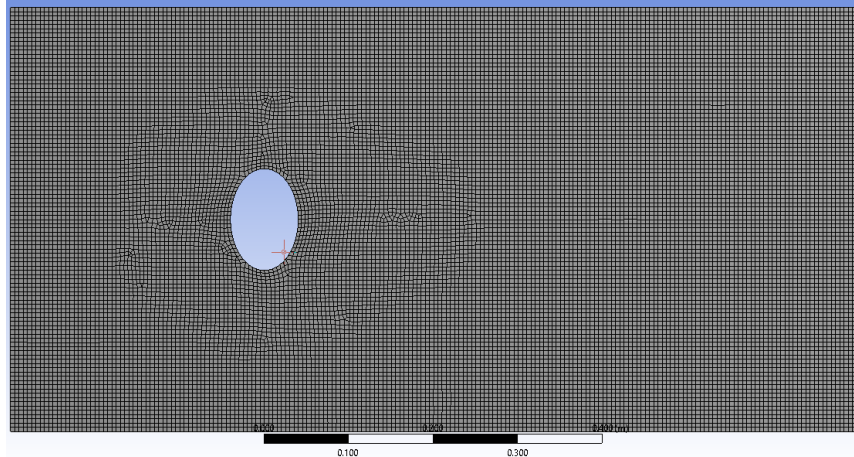

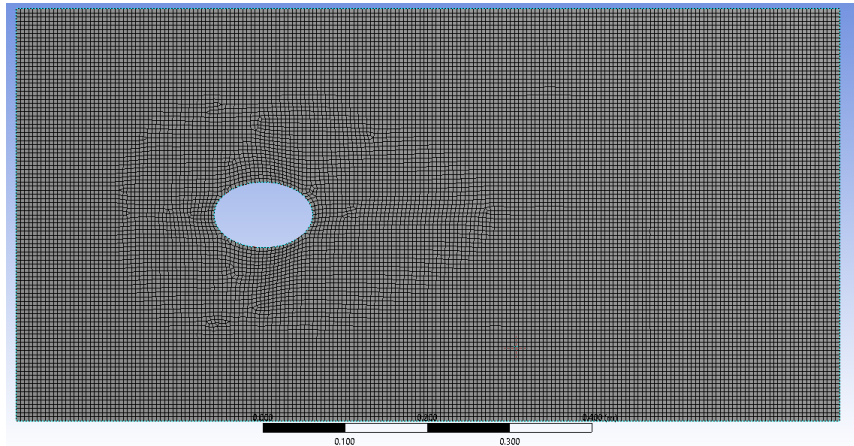Figure 5. Run 2 Mesh and Computational Domain

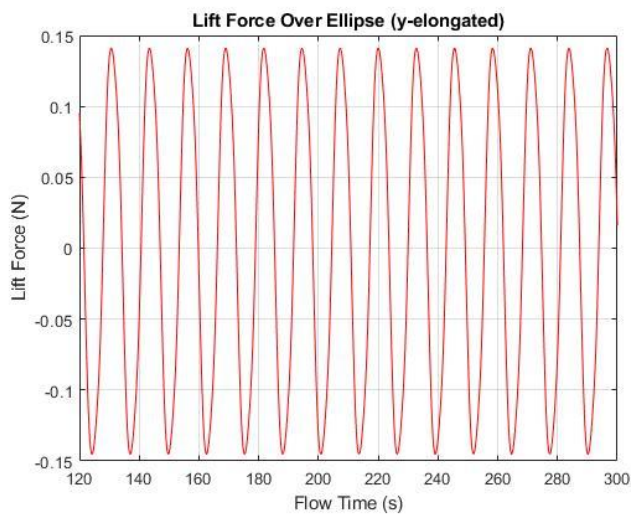Figure 6. Run 3 Mesh and Computational Domain

Figure 7. Task 1 Run 2 Lift Force vs. Time

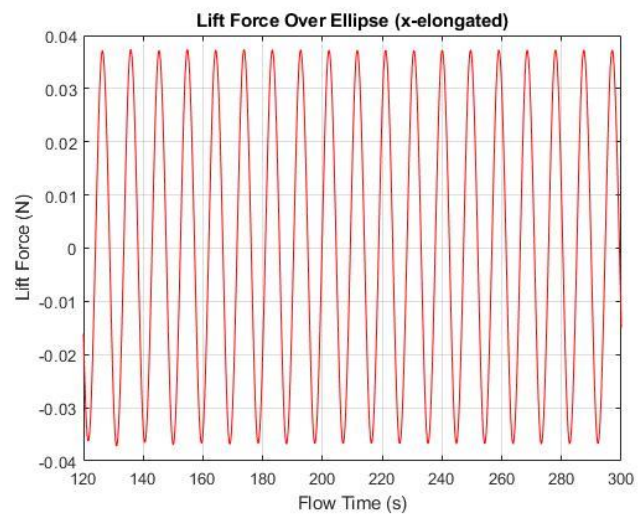Figure 8. Task 1 Run 3 Lift Force vs. Time

The results from each of the three runs are presented in table 1.

Table 1			
	Run 1 (Cylinder)	Run 2 (y-elongated ellipse)	Run 3 (x-elongated ellipse)
Amplitude (N)	0.067275	0.1432	0.03399
Period (s)	11	12.75	9.25

These results show that the amplitude and period increased when the cylinder was elongated into an ellipse along the *y*-axis while the period and amplitude decreased when the cylinder was elongated into an ellipse along the *x*-axis.

Task 2

In this task, flow over a "flying saucer" was modeled in Fluent. Unlike Task 1, a full three-dimensional simulation was used for this task. A cylindrical wind tunnel, with a velocity inlet on one side and a pressure outlet on the other was used. A parabolic velocity profile was defined for the velocity inlet as follows:

$$u = 50\left(1 - \left(\frac{r}{R}\right)^2\right)$$

Where

$$r = \sqrt{y^2 + z^2}$$

The profile of the flying saucer is defined by a geometry file. This file was imported as a 3D curve and revolved around the y-axis to create the profile. A new plane was created with the same origin as the system but rotated about the *z*-axis. This is the *y*-axis used for the geometry. Between runs, the angle at which this new plane is rotated is varied to analyze four different angles of attack. The profile of the saucer is "removed" from the computational domain through the "Boolean" function.

For the analysis, the standard k-epsilon model is utilized. The computational domain is filled with air with a constant density of
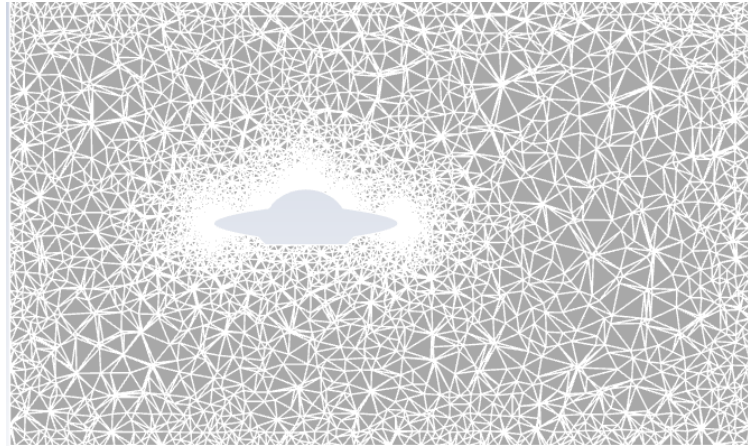

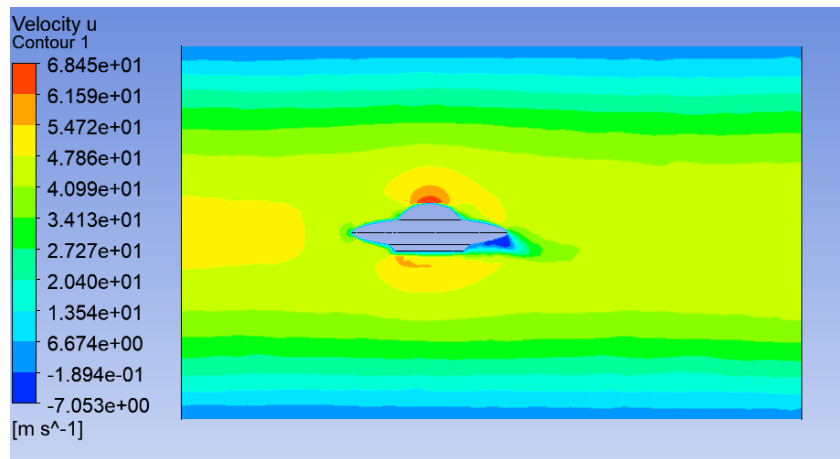Figure 9. Task 2 Mesh and Computational Domain
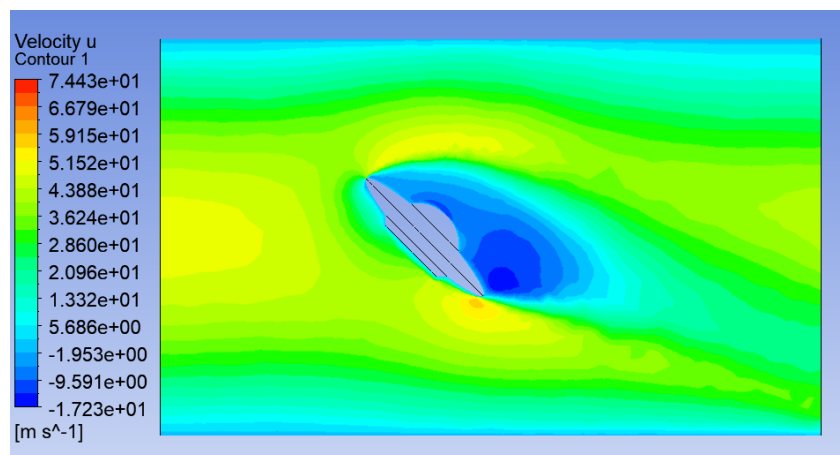

Figure 10. Task 2 *x*-Velocity Contour, θ=0°

Figure 11. Task 2 *x*-Velocity Contour, θ=45°

0.4 kg/m^3 and a viscosity of 1.4 x 10^-5 N s m^-2. Since a steady solution is sought, hybrid initialization was used for each run. Four runs are performed at tilt angles of 0, 15, 30, and 45 degrees.

The mesh used for this simulation is displayed below. For each run, an element size of 0.05m meters was used with the "capture curvature" option selected. The mesh for the 0-degree case is displayed in Figure 9, although the same mesh settings were used for each run.

Figures 10 and 11 show the *x*-velocity contours for the 0 and 45-degree cases. These plots show the parabolic velocity profile at the inlet as well as the effects of

Figure 12. Task 2 Run 2 Lift Force vs. Time

the flying saucer. Both the 0 and 45-degree cases show an acceleration of flow over the top surface of the flying saucer followed by a low, even negative velocity downstream of the saucer. It is important to note that the saucer has stalled aerodynamically in the 45-degree case. We can tell because of the flow detachment which is shown in Figure 11. The lift and drag results from the simulation also back up this observation.

For the 0, 15, and 30-degree runs, the solution converged smoothly in about 100 iterations. Monitors were placed on lift and drag force in Fluent and the simulation was run until these values were steady. Because the saucer has stalled in the 45-degree case, the flow is inherently unsteady. Therefore, a steady solution cannot be obtained. In this run, the lift and drag forces oscillated and never converged to a steady solution. This is expected as the turbulence effects result in unsteady flow under these conditions. The Lift and Drag forces as a function of iteration are plotted in Figure 12. This last run was run for 400 iterations, since the oscillations and residuals seemed to have stabilized by this point. In order to determine lift and drag forces for this run, the value of one peak and trough were determined in MATLAB. The average of these two values was then taken to be the force value for the deliverable.

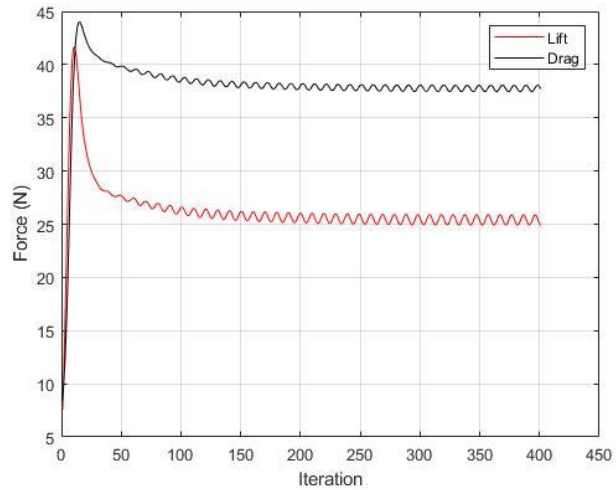The lift and drag values for each tilt angle are presented in Table 2 and plotted in Figure 13.

Table 2		
Tilt Angle (°)	Lift Force (N)	Drag Force (N)
0	4.5958	3.1337
15	24.919	6.9503
30	52.658	20.775
45	25.409	37.753

Figure 13 shows lift and drag force as a function of tilt angle. The plot shows that both lift and drag tend to increase as tilt angle increases. However, between 30 and 45 degrees, lift force drops off. This is because the surface stalls and the flow separates, increasing drag but decreasing lift. This phenomenon of stalling and flow separation was discussed earlier and is shown in Figure 11.
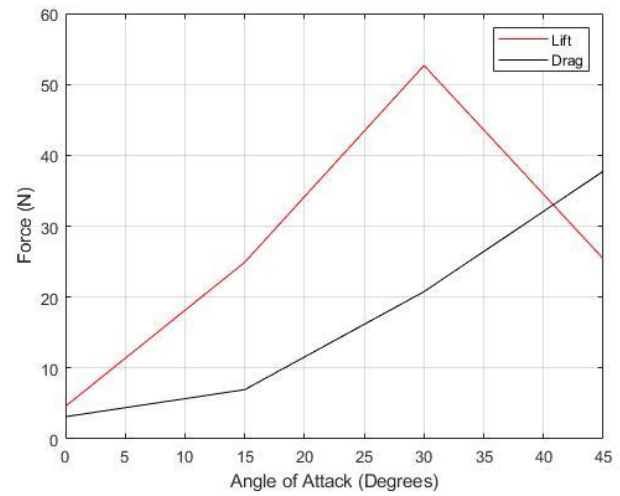

Figure 13. Task 2 Lift and Drag vs Tilt Angle

Task 3

In this task, flow is simulated over a pentagonal building in a three-dimensional domain. The domain is a rectangular prism with the pentagon in the middle. The inlet is set to a constant 50 m/s velocity. The domain is filled with air set to standard Fluent Database settings. The outlet is set to a pressure outlet and the remaining surfaces are set to walls, with a named selection being created for the walls of the building. The standard k-epsilon turbulence model is used for this analysis.

The mesh used for this analysis was set to default settings with an element size of 0.2m. I experimented with enabling inflation on the building's surface, but this yielded similar results at the expense of time. To ensure consistency and to save time and computational power, I used the standard 0.2m mesh for both runs. The mesh on the planes of interest for this task is displayed in Figure 14.
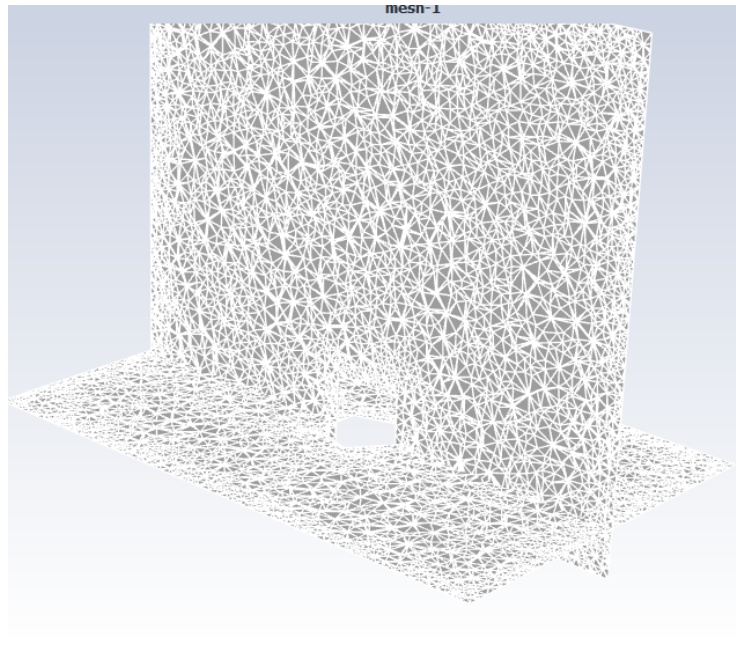

Figure 14. Task 3 Mesh and Computational Domain

Run (a)

Figures 15 and 16 show the static pressure and y-velocity on a plane 1m above and parallel to the ground, slicing through the building. Figure 17 shows the y-velocity on the plane of symmetry perpendicular to the ground. In this run, the flat side of the pentagon faces the wind. It is clear that there is a high-pressure zone on the upwind side of the pentagon and a low-pressure zone on the downwind side of the pentagon. There is a turbulent wake on the downwind side of the pentagon. The flow remains attached on three of the five sides.

The results from Fluent yielded a total drag force on the building of **3610.39 N**, **10.80 N due to viscous forces, and 3599.59 N due to pressure forces.**
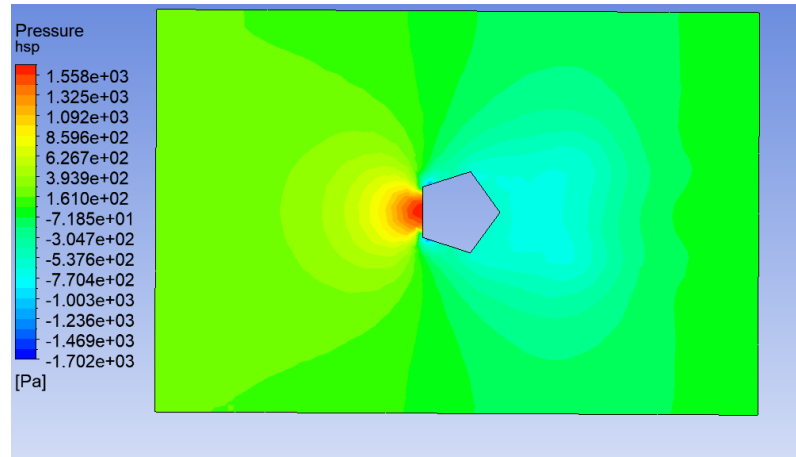

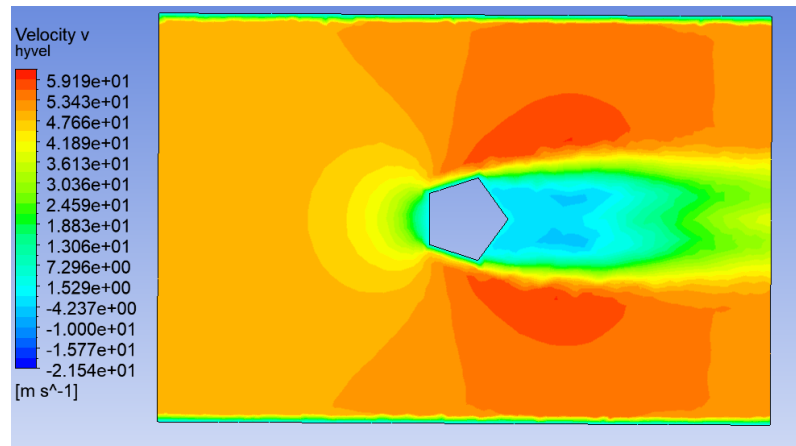Figure 15. Task 3 Run (a) Horizontal Static Pressure Contour

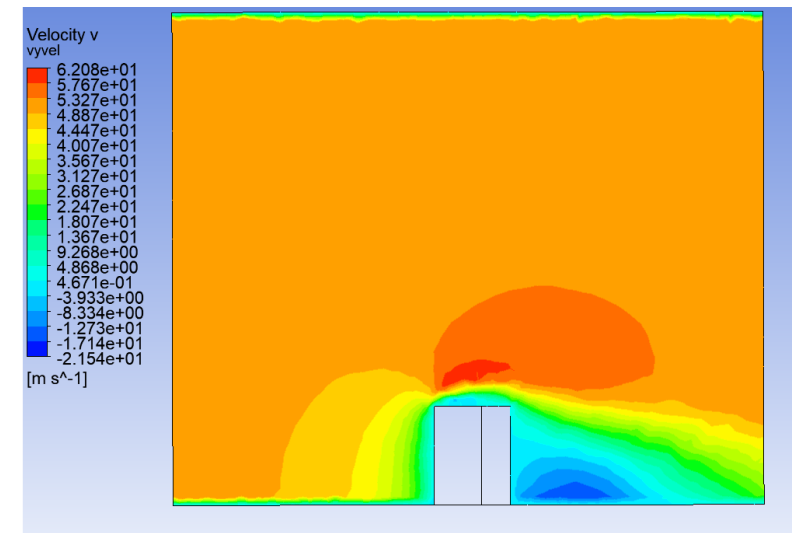Figure 16. Task 3 Run (a) Horizontal *y*-Velocity Contour

Figure 17. Task 3 Run (a) Vertical *y*-Velocity Contour

Run (b)

In this run, conditions are the same except the wind is flowing into a point of the pentagon instead of a flat side.

These results look similar to the first case. There is a high-pressure zone on the leading edge and a turbulent low-pressure wake. However, in this case, the effect of the wake is much more pronounced and the wake is much larger.

The results from Fluent report a total drag value of **5323.78 N, 1.61 N of which due to viscous forces and 5322.17 N due to pressure.**

There are distinct differences between these cases. While it might seem surprising that the sharp point produces more drag than the blunt edge, but the plots tell an interesting story. In Run (a), there is high pressure on one side and low pressure on the other four. The difference between the high-pressure blunt face and low pressure on the two downstream faces create a net drag force in the +*y* direction. However, the other two leading edge faces are in low pressure, therefore decreasing the positive *y* force. This explains why the pressure drag is so much larger in the second run. In the second run, the two
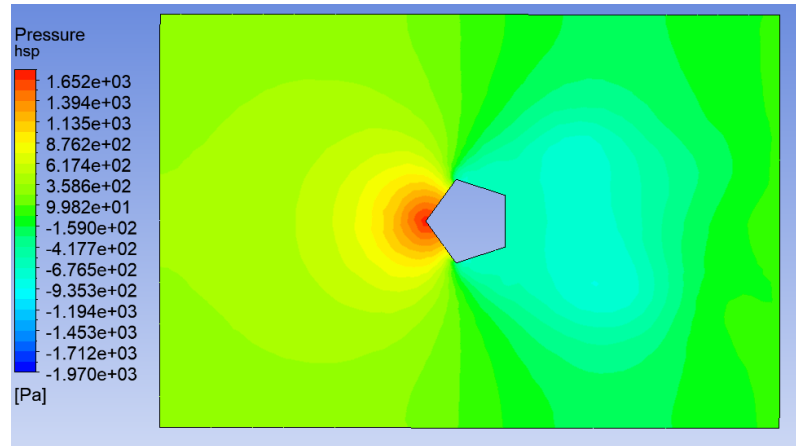

Figure 18. Task 3 Run (b) Horizontal Static Pressure Contour
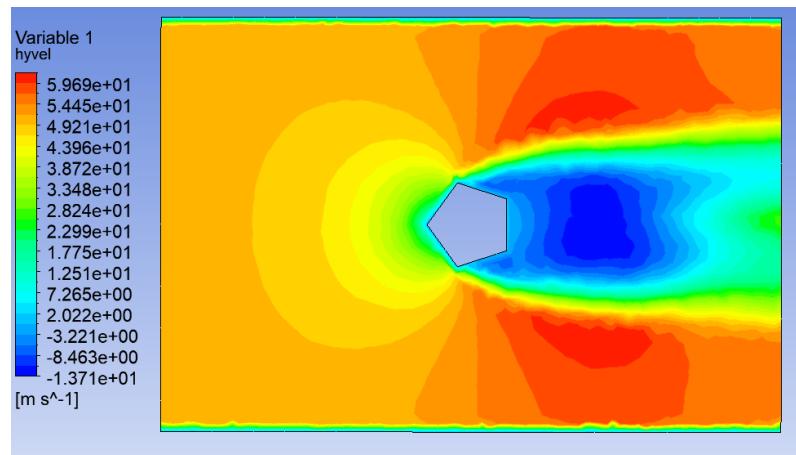

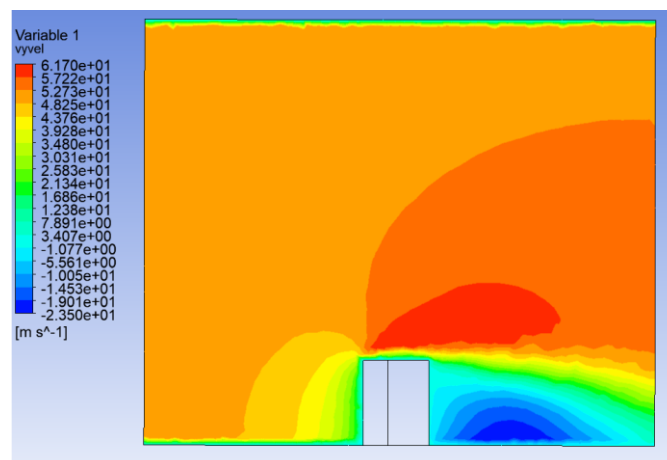Figure 19. Task 3 Run (b) Horizontal y-Velocity Contour

Figure 20. Task 3 Run (b) Horizontal Static Pressure Contour

leading edges are in a high-pressure zone and the three trailing faces are in a low-pressure zone, creating a force in the positive y direction with nothing to mitigate this force as in the first run.

The velocity profiles explain the difference in viscous drag between the two cases. In the first case, the flow remains attached on the three leading faces. Because of the no-slip condition, there is a velocity gradient in this area. This velocity gradient is steep as shown in the contour. This velocity gradient on three of the five faces explains why the viscous forces are greater in the first run. In the second run, the flow detaches, leading to a gentler velocity gradient and therefore less viscous drag.

Task 4

In this task, I am asked to repeat Task 1 with my chose of asymmetric "cylinder", if area is about the same. The goal is to see a large-amplitude response can be simulated as in Video 3 in the lecture. I ran three cases with three different geometries. The three shapes I used were a half circle, a crescent, and a triangle with rounded edges. Each shape was placed at the origin as in Task 1. All other settings are the same as Task 1. I could not obtain this response in my three runs, so I will present the data for each run. The data presented in this Task is Lift Force calculated using the automatic function in Fluent.

Run A

For this run, I simulated flow over a half cylinder as demonstrated in the video. The flat side of the semicircle is facing the wind. The diameter of this circle is 14.14 cm, which gives the same area as a circle with a diameter of 10 cm. The lift force response started to increase in the first minute of the simulation, but eventually the response returned to constant amplitude. This case did not create the desired result.
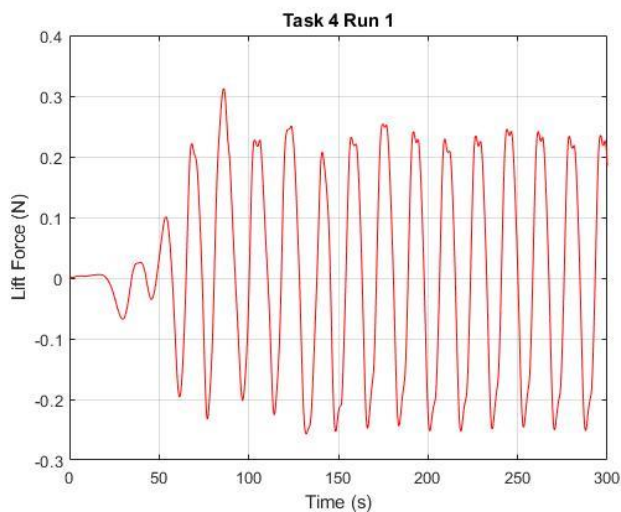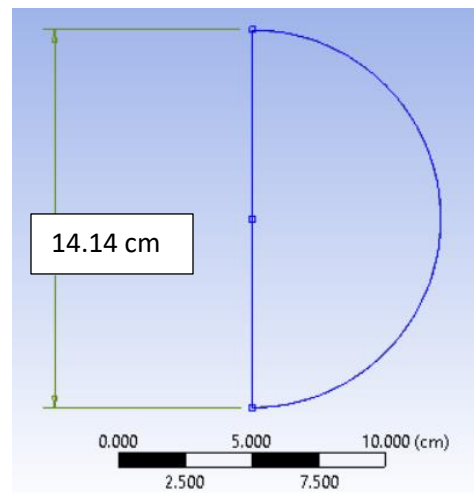

Figure 21. Task 4 Run A Lift Force vs. Time

Figure 22. Task 4 Run A Geometry

Run B

In this case, a simple crescent was used for the geometry. To create this geometry, a semicircular arc with a diameter of 16 cm was created. Then, an arc from three points was created, coincident with the ends of the semicircle. The radius of the inscribed arc is defined by the distance between the center of the arc and the origin, which is colinear with the endpoints of the semicircular arc. This dimension is defined as 16 cm. The fluid flows from left to right, into the concave part of the crescent. The results show that the period of the response is constant, but the amplitude is somewhat chaotic. While the amplitude does trend upwards, the changes in amplitude between each peak is variable and unpredictable. I do not consider this run to be a success.
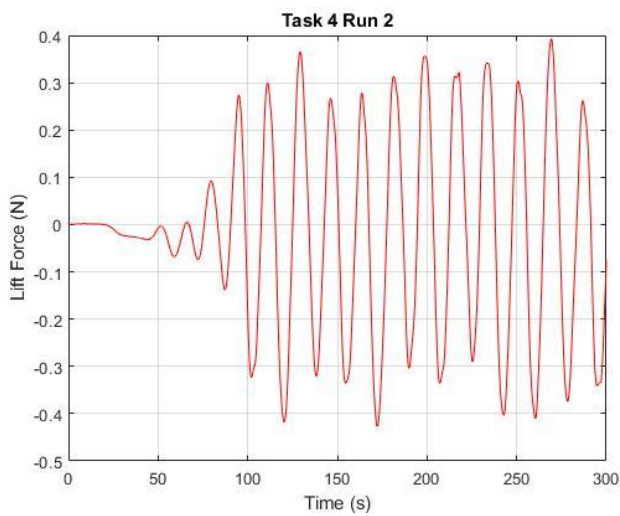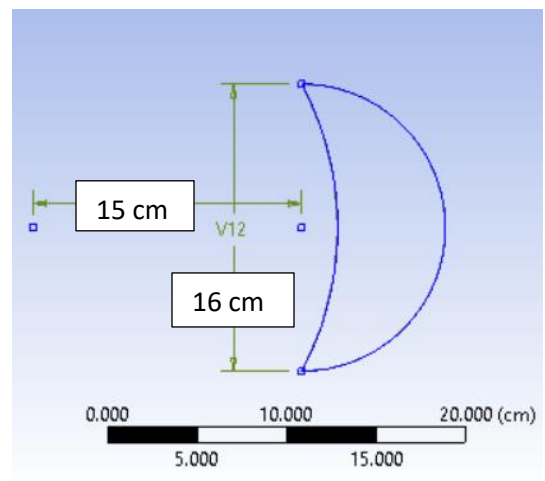

Figure 23. Task 4 Run B Lift Force vs. Time

Figure 24. Task 4 Run B Geometry

Run C

In this run, flow was simulated over an equilateral triangle with rounded corners. The base equilateral triangle has a side length of 15cm, and the corners have a radius of 1.75cm. This flow was the most regular out of all three runs. The amplitude increases nearly linearly for the first four cycles and then stays at a constant amplitude.
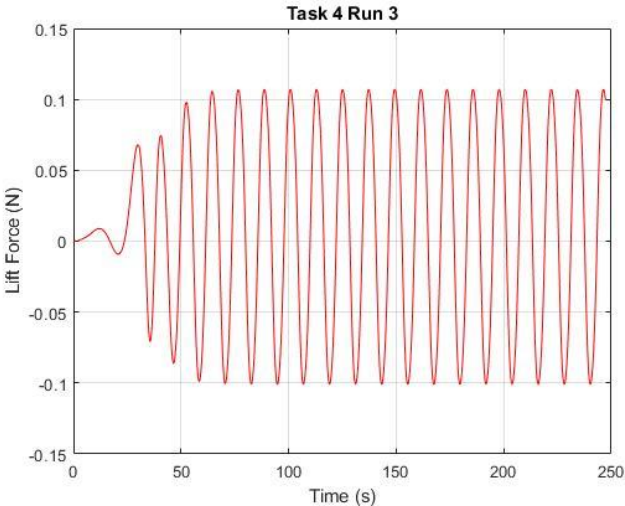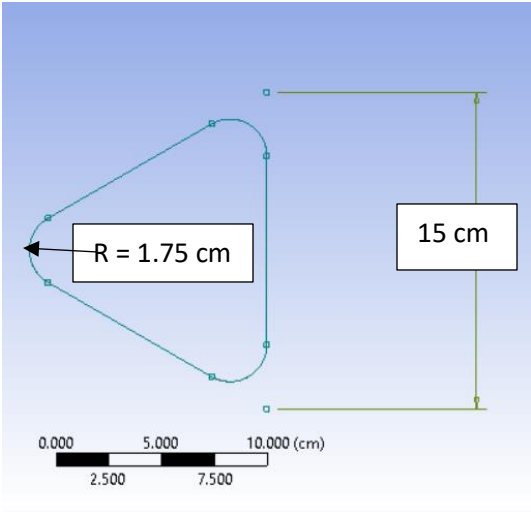

Figure 25. Task 4 Run C Lift Force vs. Time

Figure 26. Task 4 Run C Geometry